

Nonlinear Viscoelastic Predictions of Uniaxial-Extensional Viscosities of Entangled Polymers

C. Pattamaprom¹, J. J. Driscoll², and R.G. Larson^{1,*}

Department of Chemical Engineering¹, Department of Mechanical Engineering²,
University of Michigan, Ann Arbor, MI, 48109, USA

SUMMARY: A simplified version of a convective-constraint-release model by Mead, Larson, and Doi¹⁾ is used here for predicting steady-state viscoelastic properties of linear polydisperse polymers in uniaxial extensional flow. The model predictions are compared with linear dynamic viscosities and steady-state uniaxial extensional viscosities of polystyrenes for which GPC measurements of the molecular weight distribution were reported²⁾. By using parameter values obtained from data for monodisperse polystyrenes, the predictions for the polydisperse samples are made without adjustable parameters. For well-entangled samples, good agreement is obtained for both linear viscoelastic and extension-thinning regimes. For a weakly-entangled sample³⁾, a transition from extension thinning to extension thickening as the extension rate increases appears to be correctly predicted by the model. The effects of constraint release are pronounced in the stretch ratio and viscosity contribution from each component to the overall viscosity.

Introduction

The validity of the empirical Cox-Merz relationship⁴⁾ allows steady-state nonlinear viscoelastic predictions in shear flow to be obtained from measurements of linear viscoelastic properties. In fast extensional flows, however, there is no good empirical relationship between linear and nonlinear viscoelastic properties, and theoretical predictions are complicated by the stretching of polymer chains and consequent strain-hardening phenomena. Since extensional flows occur often in polymer processing industries, a good molecular model for predicting extensional flow properties is crucial.

While rheological theory for well-entangled polymers in the linear viscoelastic regime is well developed, predictions in the nonlinear regime are much less advanced due mostly to additional mechanisms arising from the large deformation of polymer chains and the complexity of nonlinear relaxation phenomena. The first detailed molecular model that is capable of predicting both linear and nonlinear rheological properties of well-entangled polymers was proposed by Doi and Edwards^{5,6)}. This model is based on the notion of reptation

in a conceptual tube of constraints imposed by the mesh of surrounding polymer molecules. While the Doi-Edwards theory successfully predicts the nonlinear rheological response of entangled polymers in step strains (i.e., the “damping function”), it still has several drawbacks in both linear and nonlinear regimes. The drawbacks include excessive shear thinning in steady-state shearing flow at moderate to high deformation rates and the lack of an overshoot in the first normal stress difference (N_1) after start up of fast shearing flows. The Doi-Edwards-Marrucci-Gritzuti (DEMG) model^{7,8)}, which is a modified version of the Doi-Edward model, tried to correct the drawbacks by including “tube stretch” into the model. Although this inclusion improves the predictions of first normal stress differences and shear stresses in the transient regime, the excessive shear thinning that occurs at steady state remains the same.

Recently, the idea of “convective constraint release (CCR)”^{9,10)} has been incorporated into the DEMG model by Mead, Larson, and Doi (1998)¹¹⁾. Convective constraint release occurs when the polymer chains composing the mesh begin to undergo their retraction processes; therefore, this mechanism is significant in fast flow, i.e. deformation rate higher than τ_d^{-1} , where τ_d is the reptation “disengagement” time. Although the convective constraint release concept is promising, numerical calculations with the full constitutive model are complicated. A simplified, or “toy”, version of the Mead-Larson-Doi (MLD) model has been developed by assuming that all parts of a polymer chain share the same stretch ratio and orientation. Although this simplification may seem severe, it seems to capture well the predictions of the full model, especially at steady state, where variations in orientation of the polymer contour are not significant.

To extend the MLD model to account for polydispersity in molecular weight, another form of constraint release, which involves reptation of surrounding chains away from the entanglement constraints, must be incorporated along with the convective constraint release. Very recently, Mead, Larson, and Doi¹⁾ combined both convective and reptative constraint release into a single, unified formalism, called the “Dual Constraint Model”. A simplified “toy” version of this model was also developed. In the linear viscoelastic limit, this toy model for a polydisperse system collapses to the “double reptation” formalism^{12,13,14)}, which has been proved successful in the prediction of linear viscoelastic properties of polydisperse polymers. The inclusion of both convective and reptative constraint release reduces the degree of shear thinning and improves the predictions at steady state. For example, the toy version of the Dual

Constraint Model predicts quite accurately the well-known Cox-Merz relationship⁴⁾ between steady-state shear viscosity and dynamic viscosity for polydisperse entangled polymers.

In this paper, we analyze the simplified, or “toy”, version of the Dual Constraint Model for polydisperse commercial polymers in steady-state uniaxial extension. The model parameters are the plateau modulus (G_N^0), the disengagement time (τ_d), the Rouse time (τ_s), and the nonlinear elastic spring constant (k_s). We investigate the contribution from each molecular weight component to the extensional viscosity and the effect of constraint release, and compare the predictions with steady-state uniaxial extensional experiments for commercial polystyrenes from Laun and Schuch²⁾ and Takahashi et al.³⁾

Theoretical Background

The equations of the “toy” Dual Constraint Model are:

$$\frac{1}{\tau_{ij}} = \frac{1}{\lambda_i^2 \tau_{d,i}} + f(\lambda_i) \left(\kappa : S_j - \frac{\dot{\lambda}_j}{\lambda_j} + \frac{1}{\lambda_j^2 \tau_{d,j}} \right) \quad (1)$$

$$S_j = \sum_k w_k \int_{-\infty}^t \frac{dt'}{\tau_{jk}(t')} \exp \left[- \int_{t'}^t \frac{dt''}{\tau_{jk}(t'')} \right] Q(E(t, t')) \quad (2)$$

$$\dot{\lambda}_i = \lambda_i \kappa : S_i - \frac{k_{s,i}(\lambda_i)}{\tau_{s,i}} (\lambda_i - 1) - \frac{1}{2} (\lambda_i - 1) \sum_j w_j \left(\kappa : S_j - \frac{\dot{\lambda}_j}{\lambda_j} + \frac{1}{\lambda_j^2 \tau_{d,j}} \right) \quad (3)$$

$$\sigma = 5G_N^0 \sum_i w_i k_{s,i} \lambda_i^2 S_i \quad (4)$$

where λ_i , the stretch ratio, is the ratio of the current length between the entanglement spacing (L_i) for chains of type i to the equilibrium tube length between the entanglement spacing (L_{eq}). S_i is the orientation tensor, κ is the deformation gradient tensor, and σ is the stress tensor. $\tau_{d,i}$ is the disengagement time, and $\tau_{s,i}$ is longest Rouse time or “stretch time”. G_N^0 is the plateau modulus and $k_{s,i}(\lambda_i)$ is the spring coefficient accounting for the extensibility of polymer chains. It equals 1 for linear springs and becomes much greater than 1 as the springs become nearly fully stretched. The subscripts i and j denote components of the molecular weight distribution having molecular weight M_i and M_j , respectively; w_i is the weight fraction of the molecular weight component i .

The universal tensor, $Q(E(t, t'))$, derived using the "independent alignment approximation", is defined as

$$Q(E(t, t')) \equiv \left\langle \frac{E(t, t') \cdot \underline{u}' E(t, t') \cdot \underline{u}'}{|E(t, t') \cdot \underline{u}'|^2} \right\rangle_0$$

where $E(t, t')$ is the deformation gradient history, \underline{u}' is a unit vector distributed randomly over the unit sphere, and $\langle \rangle$ represents an ensemble average over all \underline{u}' .

Constraint release shows up in the last terms of eq (1) and (3). Eq (1) describes the relaxation rate, which is a linear combination of the reptation rate and constraint-release rates. The first two terms in the parentheses in eq (1) are due to convective constraint release; the last term is due to reptative constraint release. Eq (3) describes stretch rate of the tubes; the stretch rate is slowed down by the same constraint-release term that appears in eq (1). CCR is believed to induce tube shortening when a polymer chain is highly stretched and to induce tube reorientation at low stretch ratios. $f(\lambda_i)$ in eq. 1, which equals $1/\lambda_i$, serves as a crossover function between the two mechanisms, the tube shortening and the tube reorientation. In the limit of linear viscoelasticity, $\lambda_i = 1$, $\kappa : S = 0$, and $Q = \frac{1}{5} \underline{\gamma}$, where $\underline{\gamma}$ is the linear-viscoelastic strain tensor. In this limit, all CCR terms vanish and this set of equations collapses to the double reptation model.

Steady-State Uniaxial Extensional Flow

This paper will explore predictions made by the Dual Constraint toy model for steady-state uniaxial extension in polydisperse mixtures of linear polymers. By applying eqs. (1)-(4), the extensional viscosity ($\bar{\eta}$), stretch ratios (λ_i), and orientation tensors (S_i) can be predicted.

For uniaxial extensions, the variables used in eqs. (1)-(4) are described as follows:

The velocity gradient tensor (κ), and the deformation tensor ($B = E^T \cdot E$) can be written

as

$$\kappa = \nabla \underline{v} = \begin{pmatrix} \dot{\epsilon} & 0 & 0 \\ 0 & -\dot{\epsilon}/2 & 0 \\ 0 & 0 & -\dot{\epsilon}/2 \end{pmatrix}; \quad B = \begin{pmatrix} \lambda^2 & 0 & 0 \\ 0 & \lambda^{-1} & 0 \\ 0 & 0 & \lambda^{-1} \end{pmatrix} \quad (5)$$

where $\dot{\epsilon}$ is the extension rate. The stretch ratio, λ , in equation (5) is a continuum quantity and is not the molecular “stretch” λ_i used in equation (1)-(4). It is a function of the past time t' and the present time t . In a uniaxial extensional flow, λ is described by

$$\lambda = \begin{cases} \exp[\dot{\epsilon}(t-t')] & ; \text{for } t' > 0 \\ \exp[\dot{\epsilon}(t)] & ; \text{for } t' < 0 \end{cases}$$

The universal tensor $\underline{\underline{Q}}$ is approximated using Curie's formula¹⁵⁾, namely

$$\underline{\underline{Q}} \approx \left(\frac{1}{J-1} \right) \underline{\underline{B}} - \left(\frac{1}{(J-1)(I_2 + 13/4)^{1/2}} \right) \underline{\underline{C}} \quad (6)$$

where $\underline{\underline{C}}$ is the Cauchy tensor, defined by $\underline{\underline{C}} = \underline{\underline{B}}^{-1}$. I_1 is the trace of the tensor $\underline{\underline{B}}$, and I_2 is the trace of the tensor $\underline{\underline{C}}$. J is related to I_1 and I_2 by $J \equiv I_1 + 2(I_2 + 13/4)^{1/2}$.

The convection rate of the mesh of entanglements, $\underline{\underline{\kappa}} : \underline{\underline{S}}$, is given by

$$\underline{\underline{\kappa}} : \underline{\underline{S}} = \begin{pmatrix} \dot{\epsilon} & 0 & 0 \\ 0 & -\dot{\epsilon}/2 & 0 \\ 0 & 0 & -\dot{\epsilon}/2 \end{pmatrix} : \begin{pmatrix} S_{11} & S_{12} & S_{13} \\ S_{21} & S_{22} & S_{23} \\ S_{31} & S_{32} & S_{33} \end{pmatrix} = \dot{\epsilon} \left(S_{11} - \frac{1}{2}S_{22} - \frac{1}{2}S_{33} \right) \quad (7)$$

The spring coefficient, k_s , is approximated by the normalized Pade' inverse langevin function¹⁶⁾ as $k_s = \frac{(3-\alpha^2)(1-\alpha^2)}{(3-\beta^2)(1-\beta^2)}$, where $\alpha = L_i/L_{\max}$ and $\beta = L_{eq}/L_{\max}$. L_{\max} , the maximum length between the entanglement spacing of polymer, is given by $L_{\max} = 0.82 l_0 n_e$, where l_0 is the backbone bond length ($= 1.54 \text{ \AA}$ for a carbon-carbon bond), and n_e , which equals 319.7 for polystyrene, is the number of backbone bonds between the entanglement spacing. L_{eq} , the equilibrium length, equals $\sqrt{C_{\infty} n_e l_0^2}$, where C_{∞} is the characteristic ratio. The value of C_{∞} is in the range of 5-10, and is 9.6 for polystyrene¹⁷⁾.

The extensional viscosity $\bar{\eta}$ and the viscosity contribution from each component $\bar{\eta}_i$ are defined as

$$\bar{\eta} = \frac{\sigma_{11} - \sigma_{22}}{\dot{\epsilon}} ; \text{ and } \bar{\eta}_i = \frac{\sigma_{11,i} - \sigma_{22,i}}{\dot{\epsilon}} , \text{ where } \sigma_i = w_i \left(5G_N^0 k_{s,i} \lambda_i^2 S_i \right).$$

Results and Discussion

We now compare the predictions of steady-state uniaxial extension from the toy model with experimental data from Laun and Schuch²⁾ for a set of commercial polystyrenes at 170 °C. These polymers are selected because their molecular weight distributions are reported,

along with rheological data for both the dynamic viscosity and the steady-state extensional viscosity. In addition, the temperature at which rheological measurements were made (170 °C) is very close to that (169.5 °C) at which linear viscoelastic data were reported for a monodisperse polystyrene samples¹⁸⁾. Thus, the relaxation time constants can be extracted from the monodisperse data, and the predictions of the polydisperse data are therefore made without adjustable parameters. The parameters for the model are the weight fractions (w_i) of each molecular weight component (M_i), the disengagement times ($\tau_{d,i}$), the Rouse times (or stretch times) ($\tau_{s,i}$), the spring coefficient (k_s), and the plateau modulus (G_N^0). The disengagement time for each molecular weight component (M_i) is obtained by applying the 3.4 power law of relaxation time with molecular weight (i.e. $\tau_{d,i} = KM_i^{3.4}$) where K is an adjustable prefactor (fig. 1). This empirical relationship fits data when M_i is larger than the critical entanglement molecular weight (M_c). Since the toy model reduces to the double reptation model at low deformations (i.e. in the linear regime), the prefactor K can be obtained by fitting the double reptation model to linear viscoelastic oscillatory-flow experiments for monodisperse polymers. Here, we fit the double reptation model with the experimental data in the terminal regime for two monodisperse polystyrenes at 169.5 °C¹⁸⁾ and we obtain $K = 8.8 \times 10^{-19}$ sec. In order to shift slightly the K value at 169.5 °C to 170 °C, we use the shift factor-temperature correlation of Majeste¹⁹⁾, and thereby find that K is shifted by 6% to $K =$

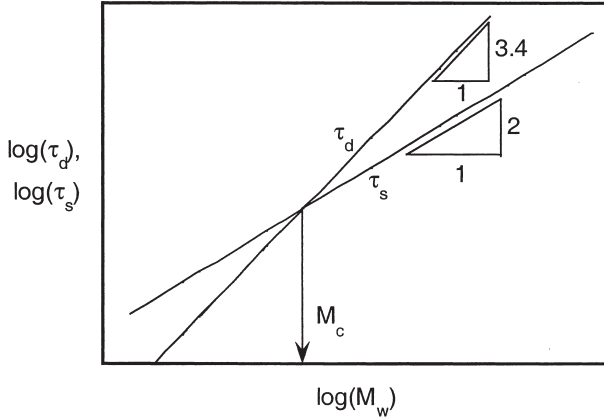


Fig. 1: The dependence of τ_d and τ_s on molecular weight. The values of τ_d and τ_s are taken to be equal to each other at $M = M_c$.

8.3×10^{-19} sec. at 170°C . The Rouse time $\tau_{s,i}$ for each component is obtained from the relationship $\tau_{s,i} \propto M_i^2$ and the equivalence of $\tau_{d,i}$ and $\tau_{s,i}$ at the critical molecular weight M_C (see fig 1). Therefore, we obtain $\tau_{s,i} = KM_c^{3.4-2}M_i^2$. Generally, M_C is $\sim 2M_e$ where M_e is the molecular weight between entanglement points. For low-molecular-weight components i.e. $M_i < M_e$, the polymer components undergo Rouse relaxation process; therefore, we set $\tau_{d,i}$ for those components to be equal to $\tau_{s,i}$. For polystyrene, $M_c \sim 35,000$ and the plateau modulus (G_N^0) is 2×10^5 Pa.¹⁷⁾

The experimental data for polystyrenes from Laun and Schuch are reported for a low molecular weight sample (PS-IV) and a high molecular weight one (PS-V). The reported M_w is 1.97×10^5 with $M_w/M_n = 1.4$ for PS-IV, and M_w is 1.3×10^6 with $M_w/M_n = 3.5$ for PS-V. The GPC curve for PS-V is given in fig. 2. By calculating the area under the GPC curve, we found slightly different M_w and M_w/M_n for both PS-IV and PS-V (i.e. $M_w = 2.05 \times 10^5$ with $M_w/M_n = 1.28$ for PS-IV, and $M_w = 1.307 \times 10^6$ with $M_w/M_n = 2.49$ for PS-V) than reported by Laun and Schuch.

To determine whether the standard double reptation and the Dual Constraint toy model can be applied to these systems, the linear viscoelastic complex viscosity (η^*) provided in fig 19 of Laun et al. is plotted against the calculated curves from the double reptation theory using

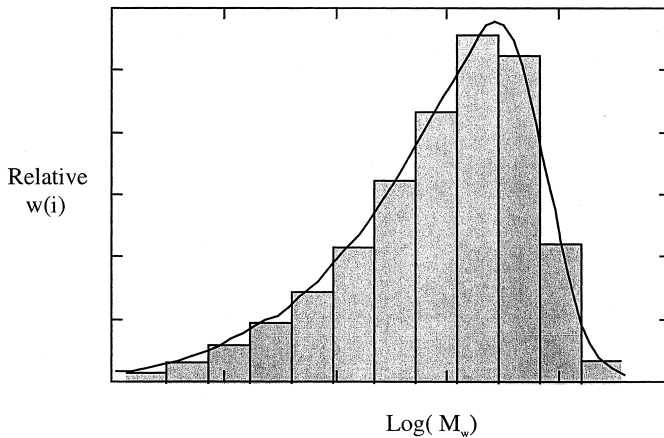


Fig. 2: Discretized molecular weight distribution of PS-V into 12 components superposed with the continuous distribution (solid line, reproduced from Laun and Schuch⁷⁾).

12-component discrete representations of the molecular weight distributions. (The results are insensitive to increasing the number of molecular weight components beyond 12.) The prediction for the 50% bimodal mixture of PS-IV and PS-V is also shown in this figure. As can be seen in fig (3), the double reptation model is adequate for PS-V; however, the prediction using the same K value is not very accurate for the low molecular weight sample (PS-IV). This discrepancy is probably caused by the inaccuracy of the tube model at low number of entanglements.

Numerical Application of the Toy Model

The curve of extensional viscosity ($\bar{\eta}$) versus extension rate at steady state calculated from the Dual Constraint toy model is compared with the experimental curve from Laun and Schuch in fig 4. As expected, the prediction for PS-IV is not as good as for PS-V and the 50% bimodal mixture, both of which are more entangled than is PS-IV. The model predicts extension thinning when the extension rate is higher than the disengagement rate, i.e. $1/\tau_d$. This decrease in viscosity is not as steep as predicted by Doi-Edward model due to the contribution from constraint release, which slows down the chain orientation in the flow

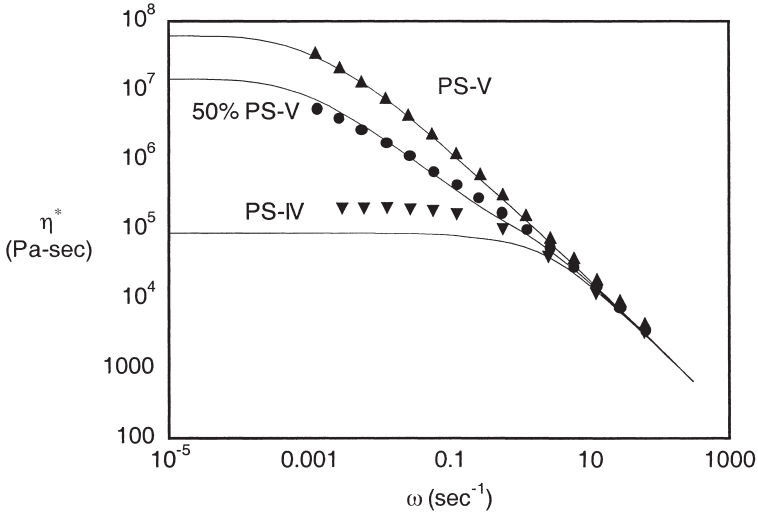


Fig.3: The complex shear viscosity determined from oscillatory shear (reproduced from Laun and Schuch²⁾ for PS-IV, PS-V, and a 50% (by weight) mixture of PS-IV and PS-V, all at 170 °C. The solid lines are the predictions from double reptation model using $G_N^0 = 2 \times 10^5$ Pa. and $\tau_d = KM^{3.4}$, where $K = 8.3 \times 10^{-18}$.

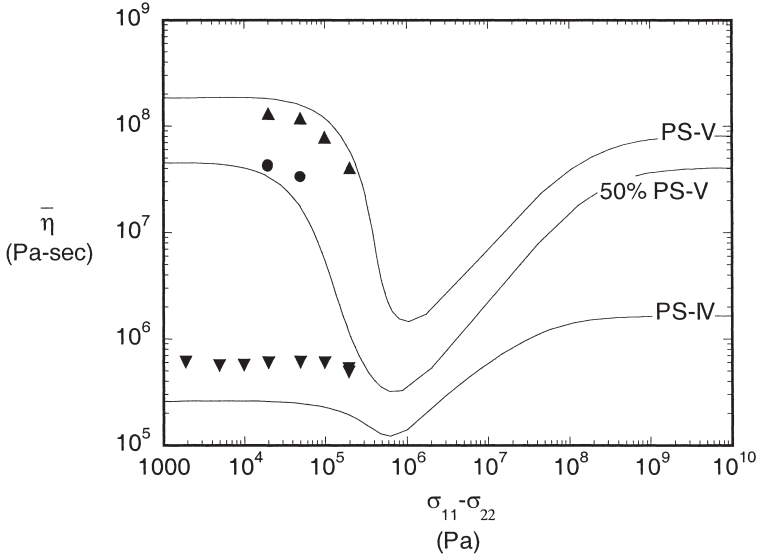


Fig. 4: The steady state extensional viscosity ($\bar{\eta}$) versus extension rate ($\dot{\epsilon}$) for PS-IV (\blacktriangledown), PS-V (\blacktriangle) and a 50% (by weight) mixture of PS-IV and PS-V (\bullet), all at 170°C. (reproduced from Laun and Schuch²⁾) The solid lines are the predictions from the toy model using $G_N^0 = 2 \times 10^5$ Pa., and $\tau_d = KM^{3.4}$, where $K = 8.3 \times 10^{-18}$ sec.

direction. The model also predicts a wider extension-thinning regime for the higher molecular weight sample; and for equal-molecular-weight polymers, the thinning regime is wider for the higher degree of polydispersity. At an extension rates of around the inverse of the average Rouse relaxation rate, $\tau_{s,av}^{-1}$, the viscosity decrease from the orientation of the polymer chains is compensated by strain hardening from the finite extensibility of the chains, creating an upturn of the viscosity. Fig (5) shows the stretch ratio $\lambda_i(\dot{\epsilon})$ for each discrete molecular weight components, superposed on a plot of the cumulative weight fraction of the stretched chains $\sum_{i=1}^{i^*} w_i$ for which extension rate $\dot{\epsilon}$ exceeds $\tau_{s,i}^{-1}$, the inverse of the stretch time. The polymer chains will stretch at lower extension rate for the longer chains, i.e. the higher molecular weights. According to fig (5), the stretching of the longest chains, which would occur at $\dot{\epsilon} \sim \tau_{s,i}^{-1}$ in a monodisperse sample, is deferred until $\dot{\epsilon}$ is high enough to stretch around 50% of all chains. Thus, constraint release causes all chains longer than the weight-averaged length to stretch at roughly the same strain rate. An analogous effect also manifests itself in the orientation tensor S_{11} - S_{22} (not shown), in which a highly-oriented state of even the highest

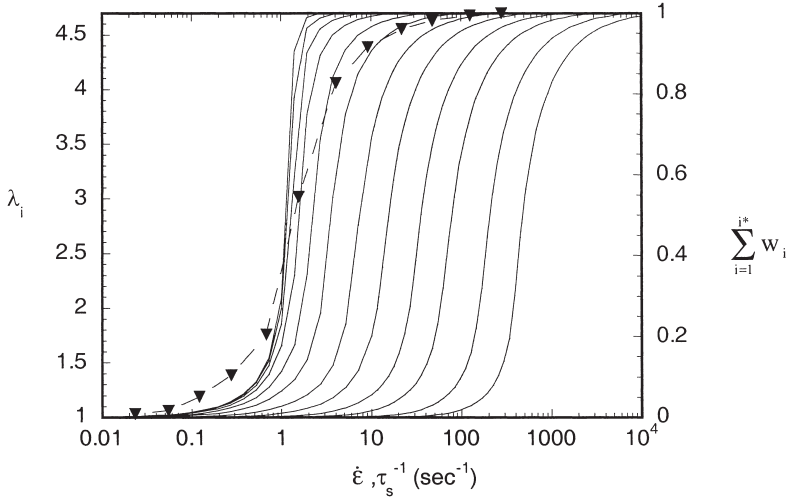


Fig. 5: Stretch ratio λ (left axis) of the 12 components (solid lines) versus extension rate $\dot{\epsilon}$ from the highest to the lowest molecular weight component (left to right) for PS-V. The symbols with the broken line indicate the cumulative weight fraction of chain i $\sum_{i=1}^{i^*} w_i$ (right axis) for which $\tau_{s,i} > \dot{\epsilon}^{-1}$ (i.e., i^* is the component i such that $\tau_{s,i} = \dot{\epsilon}^{-1}$).

molecular weight components is not reached until about 50% of the chains have started to stretch. These effects thus shift extension thickening in fig. 4 to a higher extension rate than would be the case of each chain i were to stretch when $\dot{\epsilon} > \tau_{s,i}^{-1}$ for that chain i . The viscosity contribution from each molecular weight component is also shown in fig 6. Note that extension thickening sets in at the same extension rate (around 1 sec^{-1}) for all components in the high-molecular weight half of the distribution.

Since the data from Laun and Schuch is limited to extension-thinning regime, the extension-thickening regime cannot be validated. To validate this regime, experimental data for a polystyrene sample (PS50124) from Takahashi and coworkers³ is considered here. The polymer has $M_w = 250,000$ and $M_w/M_n = 1.2$. Since the steady-state extensional viscosities were not reported, these values are extracted from plots of the transient viscosity (see fig.8 in Takahashi et al.). (We leave out the point at $\dot{\epsilon} = 0.447 \text{ sec}^{-1}$, where the steady-state value was not reached.) Since the measurements were carried out at 160°C , the prefactor K is shifted by Majeste's correlation to $2.98 \times 10^{-18} \text{ sec}$. Although the GPC curve for the polymer is not available, the narrow molecular-weight distribution of this polymer ($M_w/M_n = 1.2$) makes the

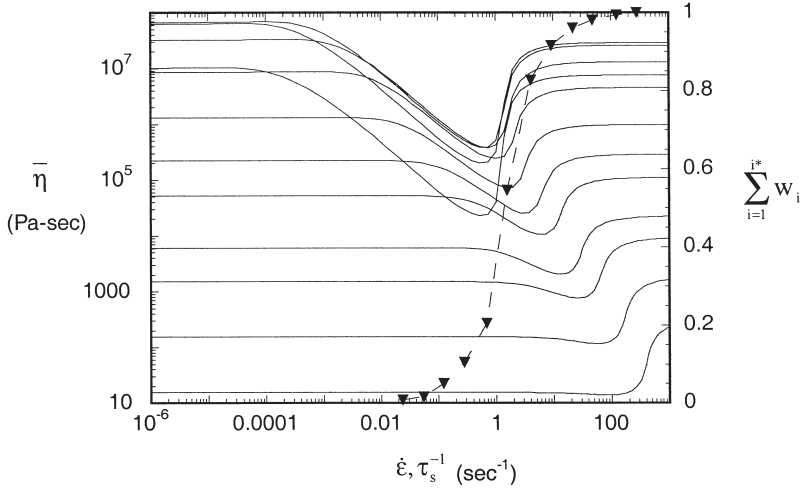


Fig. 6: Viscosity contribution from all components to the overall extensional viscosity $\bar{\eta}_i$ (left axis) for PS-V. The symbols with broken line are the same as in fig.5.

predictions insensitive to the distribution. Fig 7 compares the experimental data (symbols) with the model predictions for an assumed monodisperse distribution with molecular weight taken to be weight-average molecular weight. As can be seen, the prediction can capture well the extension-thinning and the extension-thickening regime. The prediction at small strain rate again underpredicts the data due to the low number of entanglements of this polymer sample.

Conclusion

We have analyzed the Dual Constraint toy model proposed by Mead, Larson, and Doi¹⁾ by comparing its predictions with the steady-state uniaxial extension from Laun and Schuch²⁾ and Takahashi et al.³⁾ The model parameters are the plateau modulus (G_N^0), the disengagement times ($\tau_{d,i}$), the Rouse times ($\tau_{s,i}$), and the spring coefficients ($k_{s,i}$). $\tau_{d,i}$ can be obtained by fitting the double reptation model to experimental data for monodisperse samples in the linear viscoelastic regime, and $\tau_{s,i}$ can be calculated from $\tau_{d,i}$ using molecular theory. All other parameters are taken from molecular theory and the molecular characteristics of the polymer. The orientation tensor and the stretch ratio of each component manifest the effect of constraint release. This constraint release plays an important role in attenuating the degree of extension thinning present in Doi-Edward and DEMG theories and also delays strain hardening to a

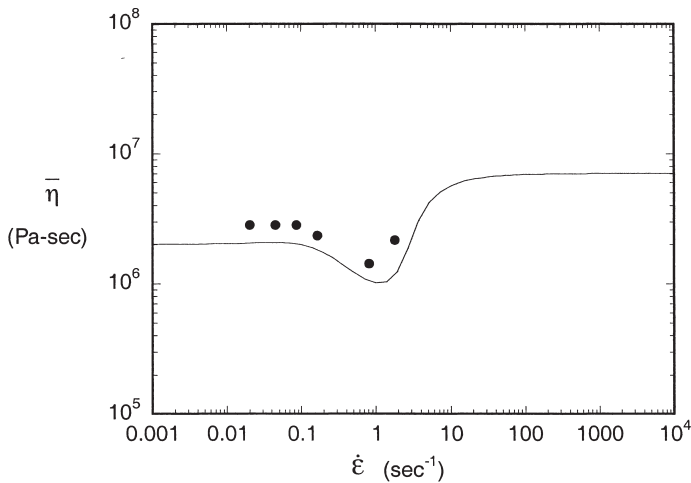


Fig 7: Steady-state uniaxial extensional viscosity versus strain rate for PS50124 at 160°C approximated from high-strain asymptotes of fig. 8 in Takahashi et al.³⁾ The line shows the toy model prediction assuming a monodisperse polymer.

higher $\dot{\epsilon}$ for the higher molecular weight components of the distribution. From a comparison of the model predictions with the experimental data, we find that the model can predict both extension-thinning and extension-thickening regimes. However, the predictions for low molecular weight polymers are still inaccurate due to the inaccuracy of tube model at low number of entanglements.

References

1. D. W. Mead, R. G. Larson, M. Doi, (1999) to be submitted.
2. H. M. Laun, H. Schuch, *J. Rheol.* **33**(1), 119 (1989)
3. M. Takahashi, T. Isaki, T. Takigawa, T. Masuda, *J. Rheol.* **37**(5), 827 (1993)
4. W. P. Cox, E. H. Merx, *J. Poly. Sci.* **28**, 619 (1958)
5. M. Doi, S. F. Edwards, *J.Chem. Soc., Faraday Trans. II.* **74**, 1789 (1978).
6. M. Doi, S. F. Edwards, *J.Chem. Soc., Faraday Trans. II.* **75**, 38-54 (1979).
7. G. Marrucci, N. Grizzuti, *Gazz. Chim. Ital.* **118**, 179 (1988)
8. D. S. Pearson, E. Herbolzheimer, N. Grizzuti, G. Marrucci, *J. Polym. Sci., Part B: Polym. Phys. Ed.* **29**, 1589 (1991)
9. G. Marrucci, *J. Non-Newtonian Fluid Mech.* **62**, 279 (1996)
10. G. Ianniruberto, G. Marrucci, *J. Non-Newtonian Fluid Mech.* **65**, 241 (1996)
11. D. W. Mead, R. G. Larson, M. Doi, *Macromolecules* **31**(22), 7895 (1998)
12. J. de Cloizeaux, *J. Europhys. Lett.* , **5**, 437 (1988)

13. C. Tsenoglou, *ACS Polym. Prepr.* **28**, 185 (1987)
14. W. H. Tuminello, *Polym. Eng. Sci.* **26**, 1339, (1986)
15. P.K. Curie, In Rheology, *Proceedings of the Eight International Congress on Rheology*, Naples, Italy (1980)
16. A. Cohen, *Rheolo. Acta* **30**, 270 (1991)
17. L. J. Fetters, D. J. Lohse, D. Richter, T. A. Witten, A. Zirkel, *Macromolecules* **27**, 4639 (1994).
18. W.W. Graessley, J. Roovers, *Macromolecules* **12**, 959 (1979)
19. J. C. Majeste, J. P. Monfort, A. Allal, G. Marin, *Rheol Acta* **37**, 486 (1998)